ISSN 0021-3640, JETP Letters, 2012, Vol. 96, No. 6, pp. 380–384. © Pleiades Publishing, Inc., 2012.
Original Russian Text © O.A. Kogtenkova, B.B. Straumal, S.G. Protasova, A.S. Gornakova, P. Zięba, T. Czeppe, 2012, published in Pis'ma v Zhurnal Eksperimental'noi i Teoreticheskoi Fiziki, 2012, Vol. 96, No. 6, pp. 419–423.

Effect of the Wetting of Grain Boundaries on the Formation of a Solid Solution in the Al–Zn System

O. A. Kogtenkova[a, *], B. B. Straumal[a, b, *], S. G. Protasova[a, *], A. S. Gornakova[a, *], P. Zięba[c], and T. Czeppe[c]

[a] *Institute of Solid State Physics, Russian Academy of Sciences, Chernogolovka, Moscow region, 142432 Russia*
** e-mail: koololga@issp.ac.ru*
[b] *National University of Science and Technology MISIS, Leninskii pr. 4, Moscow, 119049 Russia*
[c] *Institute of Metallurgy and Materials Science, Polish Academy of Sciences, 30-059 Krakow, Poland*

Received August 3, 2012

Phase transitions in the bulk and at grain boundaries in the (Al–20 wt % Zn) alloy have been studied by means of differential scanning calorimetry and transmission electron microscopy. Polycrystals with a high specific area of grain boundaries have been obtained using severe plastic deformation (high-pressure torsion). It has been shown that the Zn-based solid phase completely wets the grain boundaries in aluminum at a temperature of 200°C. The position of the grain boundary solvus line (solubility line), which is above the bulk solvus by 40–45 K, has been determined.

DOI: 10.1134/S0021364012180063

The wetting of grain boundaries by a liquid phase (melt) controls important processes of liquid phase sintering, welding, soldering, casting, etc. [1, 2]. As early as the 1970s, J.W. Cahn [3] and, almost simultaneously, C. Ebner and W.F. Saam [4] showed that a transition from incomplete wetting of free surfaces and interfaces to complete wetting is a phase transition in low-dimension systems. Then, melt-induced wetting phase transitions in grain boundaries were studied in detail both in polycrystals (see [5] and reference therein) and in specially grown [6] bicrystals with individual grain boundaries [7, 8]. The second, wetting, phase, can be not only liquid, but also solid. It has been recently shown experimentally that a solid solution of zinc in aluminum can form either a chain of particles with a nonzero contact angle $\theta > 0°$ (incomplete wetting) or a continuous layer (zero contact angle $\theta = 0°$, complete wetting) at Zn/Zn grain boundaries [9]. Aluminum particles are joined into continuous layers at temperatures above a certain T_w value. When the temperature is decreased below T_w, continuous layers are decomposed into chains of particles. A similar transition from incomplete wetting of grain boundaries in Al by the Al_3Mg_2 solid phase to complete wetting was observed with an increase in the temperature in the Al–Mg system [10].

If the wetting phase is liquid, the transition from the incomplete wetting of grain boundaries to complete wetting occurs only with an increase in the temperature because the entropy of the melt is always higher than that of the solid phase. This means that a temperature-induced decrease in the specific excess free energy σ_{SL} of the interface between the solid and liquid phases is faster than a decrease in the energy σ_{GB} of the interface between two solid phases. If the wetting phase is solid, the transition from the incomplete wetting of grain boundaries to complete wetting can occur with both an increase [9, 10] and a decrease in the temperature [11]. In particular, the experiments with aluminum-rich Al–Zn polycrystals with grains larger than 500 μm indicated that the contact angle made by zinc particles at grain boundaries in aluminum decreases with decreasing temperature and the first Al/Al grain boundaries completely covered ("wetted") by solid zinc layers appear below $T_{w0\%} = 205°C$ [12]. Below 200°C, the kinetics of change in the morphology of second-phase particles at grain boundaries, which is controlled by the bulk and grain boundary diffusion of zinc, is slowed down so much that even many-month annealing of polycrystals does not lead to a noticeable change in the morphology of particles [12].

The aim of this work is to analyze the morphology of zinc particles at grain boundaries in aluminum in samples with grains whose sizes are two or three orders of magnitude smaller than those in [12]. In such samples, not only shorter diffusion paths but also migration of grain boundaries during grain growth facilitates the achievement of the equilibrium shape of zinc particles at grain boundaries. It was previously observed how the slow migration of grain boundaries promotes the formation of their equilibrium shape in faceting–roughening transitions [13, 14]. Furthermore, it has been shown recently that the thermal effect of the transition to the complete wetting of grain boundaries

by a melt can be observed with differential scanning calorimetry (DSC) if grains are sufficiently small [15].

The Al–20 wt % Zn alloy under study was melted from high-purity components (99.9995 at % Al and 99.999 at % Zn) in a vacuum induction furnace and was cast in the form of a ∅10-mm cylinder. For experiments, 0.7-mm-thick disks were cut from an ingot. After chemical etching, disks were subjected to severe plastic deformation by the high-pressure torsion (HPT) method in Bridgeman anvils [16] at room temperature at a pressure of 5 GPa (5 turns, 1 rpm). For structure studies and calorimetric measurements, samples were cut with a diameter of 3 mm with the center in the middle of the radius of deformed HPT disks. The deformed samples were heated in a differential scanning calorimeter (TA Instruments 910 or 1600) from room temperature to 350°C at a rate of 10 and 20 K/min. Some samples were heated only to 200°C. After heating, the samples were cooled in the calorimeter to room temperature at a rate of about 10 K/s. The transmission electron microscopy study was performed with a Philips CM 20 microscope at an accelerating voltage of 200 kV. Scanning electron microscopy was performed with a Philips XL30 scanning electron microscope equipped with a LINK ISIS (Oxford Instruments) energy dispersive spectrometer.

Figure 1 shows the transmission electron microscopy micrographs of the samples after (a, b) high-pressure torsion and heating to (c, d) 200 and (e) 300°C with subsequent cooling to room temperature. The microstructure of the sample after severe plastic deformation consists of grains of almost pure aluminum (<0.5 wt % Zn) with a size of about 800 nm and pure zinc with a size of about 200 nm (Figs. 1a, 1b). At the end of heating in a differential scanning calorimeter (at 300°C), the sample consists of 20–30 μm grains of zinc solid solution in aluminum with a concentration of 20 wt % Zn. Thus, a wide minimum in DSC curves (Fig. 2) corresponds to the exothermic reaction of the complete solution of zinc in aluminum Zn + Al ⟶ (Al). It can be clearly seen from the phase diagram of Al–Zn (Fig. 3 [17]) that the phase composition of the samples after high-pressure torsion and the samples after heating in differential scanning calorimetry to 300°C corresponds to equilibrium. Below, we consider in more detail individual stages of the Zn + Al ⟶ (Al) reaction on DSC curves (Fig. 2).

According to the standard interpretation of DSC curves [18], three points can be identified in the curves in Fig. 2. The minimum at 263.0°C (for 10 K/min) or 269.6°C (for 20 K/min) corresponds to the termination of the exothermic reaction (diamonds in Fig. 3). The temperature of the onset of the exothermic reaction is the point of the intersection of the tangent to the DSC curve at the minimum toward low temperatures with the base line [18]. This temperature is 223.3 and 221.7°C for 10 and 20 K/min, respectively. These values are very close to each other; moreover, they almost coincide with the point on the solubility line (solvus) for the (Al–20 wt % Zn) alloy (marked by circles on the phase diagram in Fig. 3). For the single-stage exothermic reaction, the point of intersection of the tangent with the base line almost coincides with the temperature at which the DSC curve begins to go away from the base line downward [18]. In our case, this process begins much earlier at 202.2°C (10 K/min) and 173.0°C (20 K/min, squares in Fig. 3). This means that the observed exothermic reaction includes at least two stages. Moreover, an additional shallow wide minimum in the DSC curve is observed between 80.6 and 175.1°C in the case of heating at a rate of 10 K/min. This minimum is not observed in the curve obtained with a rate of 20 K/min. It apparently blends with the "main" maximum, which begins in this case much earlier (at 173.0°C) than in the case of heating at a rate of 10 K/min (at 202.2°C).

In order to determine the stages of the Zn + Al ⟶ (Al) reaction in our sample, we interrupted heating in differential scanning calorimetry at 200°C and rapidly cooled the sample. Its microstructure is shown in Figs. 1c and 1d. It can be seen that the size of grains increases (as compared to the state after high-pressure torsion) insignificantly (approximately by a factor of 3). However, zinc is completely redistributed in this case. Zinc is no longer concentrated in small grains at the triple junctions of aluminum grains; they are quite uniformly distributed in the form of layers at aluminum grain boundaries. It can be clearly seen that these layers are sources for zinc diffusion to the bulk of grains (it is sufficient to compare the sharp edges of zinc grains in Figs. 1a and 1b with the diffuse, smeared edges of grain boundary layers in Figs. 1c and 1d). The total content of zinc in the bulk of (Al) grains increases to about 3 wt %.

The redistribution of zinc localized after high-pressure torsion at the triple junctions of (Al) grains to layers at the (Al)/(Al) interfaces is due to the tendency of these grain boundaries to the complete wetting by zinc layers. The grains in the experiments reported in [12] were large (up to a half millimeter) and boundaries did not move upon annealing. Correspondingly, the redistribution of zinc over aluminum grain boundaries required diffusion to large distances and a huge annealing time. In this work, submicron grains grew upon annealing. Short diffusion paths and migration of boundaries during grain growth facilitated the formation of equilibrium wetting zinc layers at grain boundaries in aluminum (as the moderate migration of grain boundaries promotes the formation of their equilibrium faceting [13, 14]).

Thus, the processes manifested in DSC curves below 200°C reduce both to the redistribution of zinc particles to wetting layers over grain boundaries and to the partial solution of zinc in the bulk of aluminum grains. The Zn + Al ⟶ (Al) reaction continues with

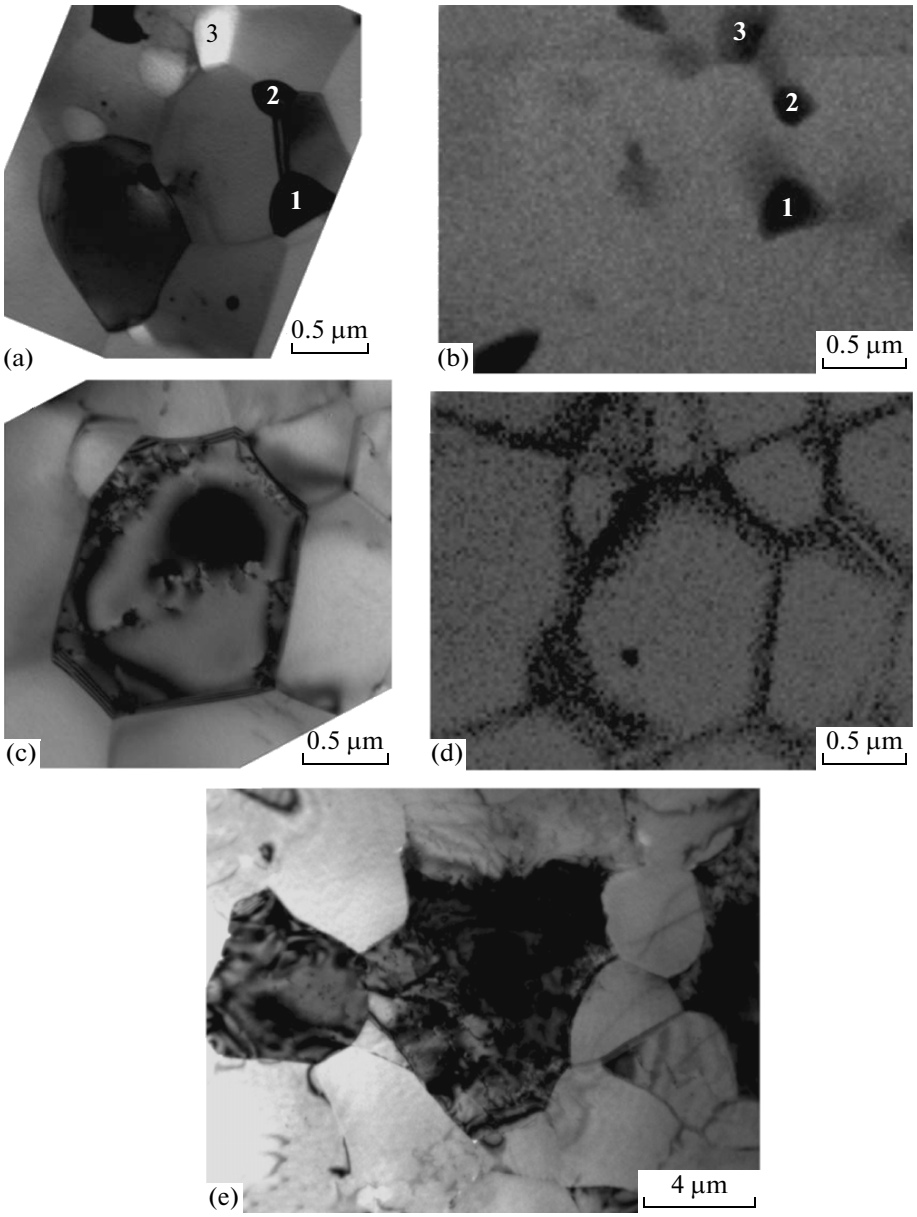

Fig. 1. (a, c, e) Microstructure of the deformed (Al–20 wt % Zn) alloy and (b, d) the zinc distribution map in the scanning transmission electron microscopy mode (a, b) for the initial sample and after the fast heating up to (c, d) 200 and (e) 300°C with subsequent fast cooling to room temperature.

further heating above 200°C. It should stop at the solvus temperature (~223°C, circles in Fig. 3). Why is this not the case and the reaction continues and stops only at 263–270°C (diamonds in Fig. 3)?

Cahn showed [3] that, if a transition from incomplete wetting of grain boundaries to complete wetting occurs at a certain temperature T_w in the two-phase area of the phase diagram, the wetting tie line should continue to the one-phase (solid solution) area of the phase diagram in the form of a so-called prewetting transition line. Since the energy of two phase interfaces $2\sigma_{SL}$ above T_w in the two-phase region is lower than the energy of the grain boundary σ_{GB} (complete wetting condition), the replacement of the grain boundary by the wetting layer leads to the following energy gain for the system:

$$\Delta = \sigma_{GB} - 2\sigma_{SL}. \quad (1)$$

This gain allows the formation of a layer of the metastable wetting phase with thickness δ at grain boundaries in the one-phase area of the phase diagram (where only the solid solution exists in the bulk in equilibrium). The formation of a phase metastable in the bulk requires the energy $g = g(c - c_s)$. This energy

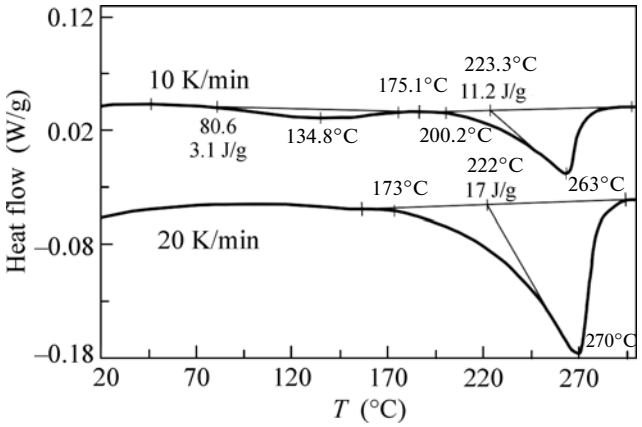

Fig. 2. Differential scanning calorimetry curves of the (Al–20 wt % Zn) alloy after high-pressure torsion at a rate of 10 and 20 K/min.

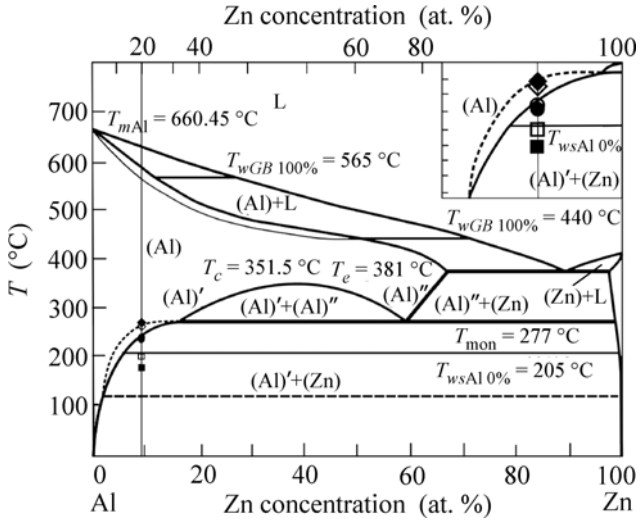

Fig. 3. Phase diagram of Al–Zn with wetting tie lines. The thick and thin lines show the bulk and grain boundary phase transitionss, respectively. The thin vertical line at 20 wt % Zn marks the studied composition. The inset shows the temperature and concentration region under study on a magnified scale. The open and filled symbols correspond to a DSC rate of 10 and 20 K/min, respectively.

is $g = 0$ when the concentration in the sample is equal to the solubility limit $c = c_s$ (on the bulk solidus line) and increases with $c - c_s$. The thickness of the prewetting layer δ can be determined from the relation

$$\sigma_{GB} - 2\sigma_{SL} = g\delta. \quad (2)$$

When δ at a certain c_b value becomes smaller than the interatomic distance, the prewetting layer disappears. Thus, the prewetting layer exists in the concentration range $c_b - c_s$. The line $c_b(T)$ is called the GB solidus or solvus. For the case where the wetting phase is liquid (i.e., between the bulk and grain boundary solidus lines), wetting layers were often observed in metals [19–23] and ceramics obtained by the liquid phase sintering method [24–40]. The zinc-containing melt in the Al–Zn system wets grain boundaries in aluminum (see Fig. 3). This process begins at $T_{w0\%}$ = 440°C for the grain boundary with the highest energy and finishes at $T_{w100\%}$ = 565°C for the grain boundary with the lowest energy [41]. The tie lines of liquid phase wetting continue into the one-phase (Al) solid solution area. Points on the grain boundary solidus were experimentally obtained with transmission electron microscopy [42] and differential scanning calorimetry [15]. The position of the grain boundary solvus (when the wetting phase is solid) was similarly obtained in this work (from the splitting of the minimum in the DSC curve, see the dotted line in Fig. 3).

To summarize, it has been shown that the zinc-based solid phase completely wets grain boundaries in aluminum at a temperature of 200°C in the samples with submicron grains. The position of the grain boundary solvus line (solubility line) in the Al–20 wt % Zn alloy has been determined for the first time by means of differential scanning calorimetry.

This work was supported by the Russian Foundation for Basic Research (project no. 11-03-01198), jointly by the Russian and Polish Academies of Sciences (bilateral cooperation program), by the Council of the President of the Russian Federation for Support of Young Scientists and Leading Scientific Schools (project no. MK-3748.2011.8), and by Narodowe Centrum Nauki (grant no. UMO-2011/01/M/ST8/078822).

REFERENCES

1. B. Straumal and W. Gust, Mater. Sci. Forum **207**, 59 (1996).
2. B. Straumal and B. Baretzky, Interf. Sci. **12**, 147 (2004).
3. J. W. Cahn, J. Chem. Phys. **66**, 3667 (1977).
4. C. Ebner and W. F. Saam, Phys. Rev. Lett. **38**, 1486 (1977).
5. N. Eustathopoulos, Int. Met. Rev. **28**, 189 (1983).
6. V. N. Semenov, B. B. Straumal, V. G. Glebovsky, et al., J. Cryst. Growth **151**, 180 (1995).
7. B. B. Straumal, W. Gust, and T. Watanabe, Mater. Sci. Forum **294**, 411 (1999).
8. B. B. Straumal, W. Gust, and D. A. Molodov, Interf. Sci. **9**, 127 (1995).
9. G. A. Lopez, E. J. Mittemeijer, and B. B. Straumal, Acta Mater. **52**, 4537 (2004).
10. B. B. Straumal, B. Baretzky, O. A. Kogtenkova, et al., J. Mater. Sci. **45**, 2057 (2010).
11. B. B. Straumal, O. A. Kogtenkova, A. B. Straumal, et al., J. Mater. Sci. **45**, 4271 (2010).
12. S. G. Protasova, O. A. Kogtenkova, B. B. Straumal, et al., J. Mater. Sci. **46**, 4349 (2011).
13. B. B. Straumal, S. A. Polyakov, E. Bischoff, et al., Interf. Sci. **9**, 287 (1995).

14. B. B. Straumal, B. Baretzky, O. A. Kogtenkova, et al., J. Mater. Sci. **47**, 1641 (2012).
15. B. B. Straumal, O. A. Kogtenkova, S. G. Protasova, et al., J. Mater. Sci. **46**, 4243 (2012).
16. R. Z. Valiev and T. G. Langdon, Prog. Mater. Sci. **51**, 881 (2006).
17. *Binary Alloy Phase Diagrams*, Ed. by T. B. Massalski (ASM International, Materials Park, 1993).
18. J. A. Dean, *The Analytical Chemistry Handbook* (McGraw Hill, New York, 1995), Standards ASTM D 3417, ASTM D 3418, ASTM E 1356, ISO 11357.
19. B. B. Straumal, O. I. Noskovich, V. N. Semenov, et al., Acta Metall. Mater. **40**, 795 (1992).
20. J. Scholhammer, B. Baretzky, W. Gust, et al., Interf. Sci. **9**, 43 (2001).
21. L. S. Chang, E. Rabkin, B. B. Straumal, et al., Def. Diff. Forum **156**, 135 (1997).
22. V. K. Gupta, D. H. Yoon, H. M. Meyer, et al., Acta Mater. **55**, 3131 (2007).
23. J. Luo, V. K. Gupta, D. H. Yoon, et al., Appl. Phys. Lett. **87**, 231902 (2005).
24. J. Luo J. Dillon, and M. P. Harmer, Microsc. Today **17**, 22 (2009).
25. J. Cho, C. M. Wang, H. M. Chan, et al., J. Mater. Sci. **37**, 59 (2002).
26. S. J. Dillon, M. Tang, W. C. Carter, et al., Acta Mater. **55**, 6208 (2007).
27. S. J. Dillon and M. P. Harmer, Acta Mater. **55**, 5247 (2007).
28. S. J. Dillon and M. P. Harmer, J., Eur. Ceram. Soc. **28**, 1485 (2008).
29. G. Pezzotti, A. Nakahira, and M. Tajika, J. Eur. Ceram. Soc. **20**, 1319 (2000).
30. Y. Furukawa, O. Sakurai, K. Shinozaki, et al., J. Ceram. Soc. Jpn. **104**, 900 (1996).
31. M. Elfwing, R. Osterlund, and E. Olsson, J. Am. Ceram. Soc. **83**, 2311 (2000).
32. H. Wang and Y.-M. Chiang, J. Am. Ceram. Soc. **81**, 89 (1998).
33. I. Tanaka, H. J. Kleebe, M. K. Cinibuluk, et al., J. Am. Ceram. Soc. **77**, 911 (1998).
34. M. Baram and W. D. Kaplan, J. Mater. Sci. **41**, 7775 (2006).
35. M. Baram, D. Chatain, and W. D. Kaplan, Science **332**, 206 (2011).
36. C. Scheu, G. Dehm, and W. D. Kaplan, J. Am. Ceram. Soc. **84**, 623 (2001).
37. A. Avishai and W. D. Kaplan, Acta Mater. **53**, 1571 (2005).
38. A. Avishai, C. Scheu, and W. D. Kaplan, Acta Mater. **53**, 1559 (2005).
39. A. Avishai and W. D. Kaplan, Zt. Metallkde **95**, 266 (2004).
40. M. Baram, S. H. Garofalini, and W. D. Kaplan, Acta Mater. **59**, 5710 (2011).
41. B. B. Straumal, A. S. Gornakova, O. A. Kogtenkova, et al., Phys. Rev. B **78**, 054202 (2008).
42. B. B. Straumal, A. A. Mazilkin, O. A. Kogtenkova, et al., Philos. Mag. Lett. **87**, 423 (2007).

Translated by R. Tyapaev